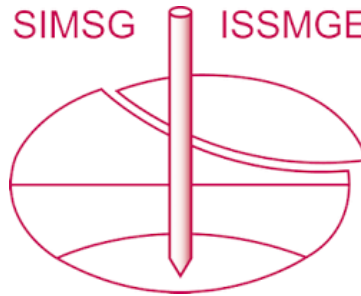


# INTERNATIONAL SOCIETY FOR SOIL MECHANICS AND GEOTECHNICAL ENGINEERING



*This paper was downloaded from the Online Library of the International Society for Soil Mechanics and Geotechnical Engineering (ISSMGE). The library is available here:*

<https://www.issmge.org/publications/online-library>

*This is an open-access database that archives thousands of papers published under the Auspices of the ISSMGE and maintained by the Innovation and Development Committee of ISSMGE.*

*The paper was published in the proceedings of the 10th International Conference on Physical Modelling in Geotechnics and was edited by Moonkyung Chung, Sung-Ryul Kim, Nam-Ryong Kim, Tae-Hyuk Kwon, Heon-Joon Park, Seong-Bae Jo and Jae-Hyun Kim. The conference was held in Daejeon, South Korea from September 19<sup>th</sup> to September 23<sup>rd</sup> 2022.*

## Centrifuge modelling of rainfall infiltration into the soil affected by rainfall and soil characteristics

K. Ono, R. Saeki & M. Okamura

*Graduate School of Science and Engineering, Ehime University, Japan*

**ABSTRACT:** For the advancement of methods used to detect signs of rainfall-induced surface failure, a better understanding of the process of rainwater infiltration into the soil is necessary. This paper presents the results of a series of vertical infiltration tests using a rainfall simulator in a centrifuge. The vertical infiltration behavior of rainwater into uniform horizontal ground was examined by varying the soil permeability, and rainfall intensity. The measurement of pore water pressure at each depth in the centrifuge enabled an accurate and rapid understanding of rainwater infiltration of rainwater in unsaturated soil. The sand layer through which the phreatic surface passed was not completely saturated at any depth and maintained a suction pressure of 1–6 kPa. There was a correlation between the ratio of the coefficient of saturated permeability to rainfall intensity and the suction of sand and the infiltration rate of rainwater.

**Keywords:** rainfall, permeability, infiltration, centrifuge

### 1 INTRODUCTION

In recent years, landslides have become more common worldwide owing to the intensification of rainfall caused by climate change; this has resulted in significant damage to our lives and infrastructure. Rainfall-induced surface failure are triggered by rainfall infiltration into the soil surface of the slope. Infiltrated rainwater increases the water content of the soil, causing an increase in the weight of the soil mass and a decrease in the matric suction of unsaturated soil, followed by soil deformation (Kitaura and Sako, 2010). When modelling of landslides and analyzing of soil deformation and failure is performed, the stress level of the soil is usually considered. Full-scale physical models can accurately define the stress state; however, the preparation of these models is costly and time consuming. Conversely, geotechnical centrifuge modelling can be performed repeatedly with high reproducibility and at a relatively low cost. Because simulating rainfall within a centrifuge is an effective experimental tool that can be used to evaluate rainfall infiltration and slope failure simultaneously, a number of studies based on centrifuge modelling have been conducted to evaluate slope stability (e.g., Zhang et al., 2011).

To establish a method to detect the signs of surface failure due to rainfall, it is necessary to better understand the process of rainfall infiltration that triggers failures. In recent years, the relationship between the volumetric water content and the initiation of slope failure has been studied. Iwata et al. (2014) showed that the development of unsaturated slope deformation correlates with changes in suction pressure and volumetric water content based

on field measurements. Consequently, Koizumi et al. (2019) proposed a prediction method for slope failure based on volumetric water content during rainfall infiltration. However, there is a lack of clarity regarding the relationship between rainfall infiltration and changes in soil water content. In particular, the effects of rainfall intensity and soil permeability on the decrease in suction and infiltration rate of rainwater into the soil need to be evaluated.

In this study, we focused only on the infiltration behavior of rainwater and conducted a series of vertical infiltration tests on uniform horizontal ground using a rainfall simulator in a centrifuge. The vertical infiltration behavior of rainfall was examined by varying the soil permeability, rainfall intensity, and rainwater viscosity.

### 2 EXPERIMENTAL METHODOLOGIES

#### 2.1 Scaling Laws

Table 1 summarizes the major scaling laws for rainfall modelling for the  $1/N$  scale model at the  $Ng$  level.

Because the main purpose of the experiment using a rainfall simulator is to observe the infiltration of rainwater and subsequent soil deformation, the time scaling of seepage is generally applied to that of rainfall. Therefore, the rainfall duration at the model scale was considerably reduced to  $1/N^2$ . The scaling of rainfall intensity was obtained from using precipitation and rainfall duration. A  $1/N$  scale model must replicate the original rainfall intensity  $N$  times in the centrifuge.

The droplet size is related to its falling velocity, which affects the impact pressure on the ground surface. Because a high impact pressure causes excessive erosion

of the ground surface, it is necessary to spray a mist of water with an appropriate size of 20  $\mu\text{m}$  (Tamate, 2010).

Table 1. Centrifuge scaling laws.

Parameter	Mode/Prototype	Dimensions
Precipitation	1/N	L
Rainfall intensity	N	$LT^{-1}$
Time (seepage)	$1/N^2$	T
Time (rainfall)	$1/N^2$	T

## 2.2 Rainfall Simulation System

A series of experiments was conducted using a geotechnical beam centrifuge at Ehime University. The radius from the axis of the centrifuge to the top of the platform surface is 1.55 m.

Fig. 1 shows the overview of the experimental setup. Eight spray nozzles (BIM series, H. Ikeuchi & Co., Ltd.) were arranged in series on a soil container. Pressurized air and liquid were supplied to the nozzles through separate systems via a rotary joint from air compressors installed outside the centrifuge to spray a fine mist. The diameter of the mist was approximately 20  $\mu\text{m}$  as per the manufacturer's specifications. The solenoid valves installed in each route were remotely operated to control the start and stop of liquid spraying. Rainfall intensity was adjusted by regulating the magnitude of the external pressure of each supply.

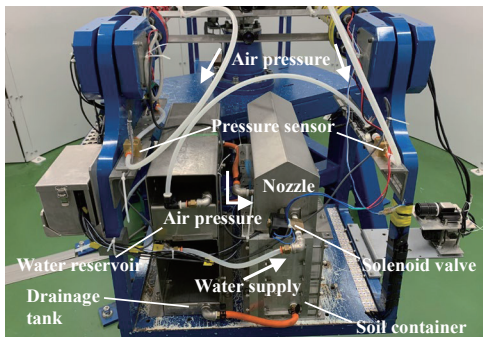


Fig. 1. Experimental setup.

Droplets released from the nozzles in the centrifugal rotational field reach the ground surface travelling along a curve owing to the Coriolis force acting on a moving object in a rotating coordinate system. The trajectory of the droplets was calibrated by tilting the nozzles in the rotational direction of the centrifuge. Fig. 2 shows the distribution of rainfall intensity for a target intensity of 60 mm/h obtained by conducting preliminary tests using 30 small measuring cups. Although there was some variation in the width direction, the rainfall intensity in the length direction of a soil container directly under the nozzles was generally uniform. In this study, the rainfall intensity measured just below the nozzles was used to evaluate the infiltration behavior because each sensor was buried just below the nozzles.

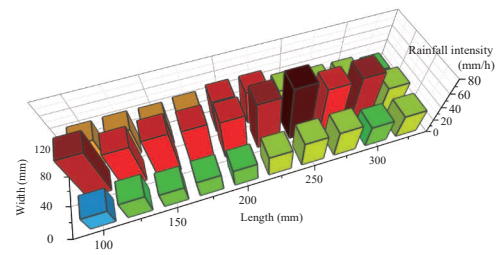


Fig. 2. Distribution of rainfall intensity at 40g.

## 2.3 Model Configuration

The schematic of the experimental model is shown in Fig. 3. Uniform horizontal ground to a depth of 8 cm was prepared in the soil container. Tohoku-Keisa No.8 sand, whose permeability was adjusted by using fine fraction content, was used. The sand was compacted into four layers to achieve a relative density of 80% with the water content of 15%. Pore pressure transducers (PAA-2Mi, Keller) that can measure matric suction, and a soil moisture meter (WD-3, Fieldpro) that measures volumetric water content were embedded in the sand deposits. Air holes were provided on both sides of the container to suppress the generation of pore air pressure due to rainfall infiltration.

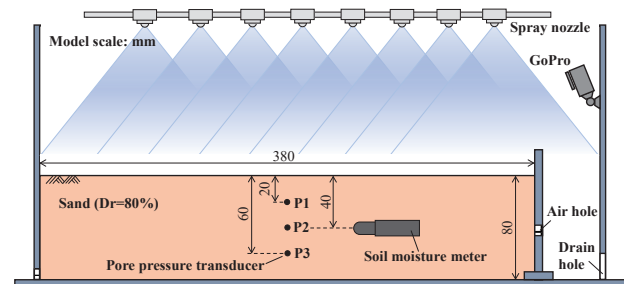


Fig. 3. Model setup.

## 2.4 Test Cases

The test cases are summarized in Table 2. In Cases-1, 2, and 3, the ratio of the coefficient of saturated permeability to the rainfall intensity (hereinafter called the relative permeability index  $I_r$ ) varies. The higher the index, the higher is the ability of the sand deposit to infiltrate rainwater. In Cases-4 and 1, the permeability and rainfall intensity are increased by the same ratio. In Case-5, a viscous fluid prepared using a metolose solution was used as a spray liquid to decrease the permeability of the sand deposit. In Cases-4 and 5,  $I_r$  is almost the same as in Case-1.

Unless otherwise noted, experimental results are shown in prototype scale.

Table 2. Test conditions.

Test ID	Coeff. of permeability $k$ (m/s)	Pore fluid viscosity $\nu$ (cSt)	Rainfall intensity $r$ (mm/h)	Relative permeability index $I_r$ (-)
Case-1	$2.4 \times 10^{-5}$	1	5	16.9
Case-2	$9.3 \times 10^{-5}$	1	60	5.6
Case-3	$2.4 \times 10^{-5}$	1	60	1.4
Case-4	$9.3 \times 10^{-5}$	1	20	16.7
Case-5	$9.3 \times 10^{-5}$	4	5	16.7

### 3 RESULTS AND DISCUSSION

#### 3.1 Rainwater Infiltration Process

Fig. 4 shows the time histories of the volumetric water content and pore water pressure during water spraying in Case-1. The water content calculated using the initial volumetric water content ( $\theta_0 = 0.2$ ) and initial void ratio ( $e_0 = 0.85$ ) was approximately 14%, which is almost consistent with the water content when the model was prepared. A pore pressure of 0 kPa indicates atmospheric pressure, and the absolute value of the negative pore pressure represents the suction of the sand.

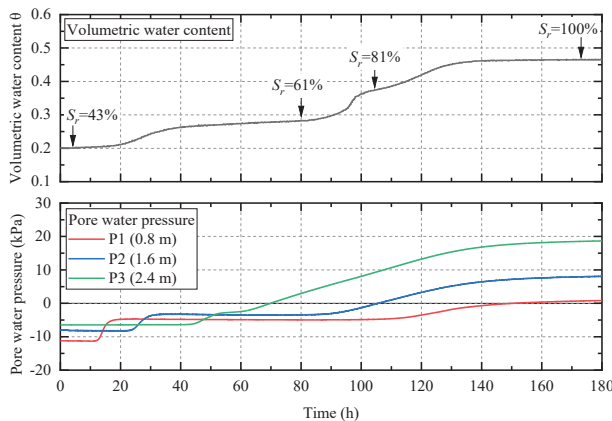


Fig. 4. Time histories of volumetric water content and pore pressure.

Approximately 20 h after the initiation of spraying, the volumetric water content increased with the descent of the phreatic surface. During this period, a small amount of pore air was entrapped in the sand (i.e., quasi-saturated state), and the increase in volumetric water content slowed for approximately 50 h. After that, the phreatic surface reached the bottom of the container and reversed, causing the groundwater level to increase. Correspondingly, the volumetric water content also increased. In this process, the entrapped air disappeared, and the degree of saturation finally reached 100%.

The pore water pressure responded in order from the surface as the phreatic surface descended. Next, each pore pressure temporarily stopped increasing, similar to the volumetric water content. In this state, the pore water pressure remained negative regardless of the depth. The pore water pressure increased again as the groundwater

level increased and showed a positive value when the surrounding area of the sensor was completely saturated. Thereafter, the pore water pressure continued to increase because of the increase in the hydrostatic pressure.

As mentioned earlier, the measurement of pore water pressure at each depth in the centrifuge enabled us to understand the infiltration behavior of rainwater in unsaturated soil in a very short time, according to the scaling law shown in Table 1.

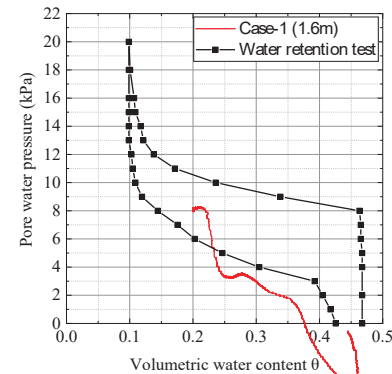


Fig. 5. Soil water characteristic curve.

Fig. 5 shows the relationship between the volumetric water content measured using the soil moisture meter and the suction of P2 at the same depth. The soil water characteristic curve obtained by conducting a water retention test is overlapped on the graph.

The relationship curve obtained by conducting the centrifuge test and the adsorption curve obtained by conducting the water retention test were in relatively good agreement. However, at low suction, the volumetric water content obtained in the centrifuge test was less than that obtained in the water retention test due to the characteristics of the measuring sensor. The pore pressure transducer measured the suction at a specific point, whereas the soil moisture meter measured the average volumetric water content around the sensor. From this point of view, measuring the water content at a specific point using a general small moisture meter is difficult in small-scale model tests such as centrifuge tests. Therefore, in the following sections, the soil moisture condition is analyzed using the soil water characteristic curve and the measured pore water pressure.

#### 3.2 Influence of Rainfall Intensity and Permeability

Fig. 6 shows the relationship between the relative permeability index and suction for all test cases. As shown in Fig. 6 (a), the deeper the sand layer, the smaller the initial suction, indicating a higher degree of saturation. This shows that the distribution of the initial volumetric water content was not uniform because of the vertical downward movement of the pore water with increase in centrifugal acceleration. However, the



difference in suction in the depth direction decreases under the quasi-saturated condition, as shown in Fig. 6 (b), implying that once the sand layer is infiltrated, the water content will be almost the same, regardless of the initial condition. The quasi-saturated suction is more correlated with the relative permeability index than with the depth. The smaller the index, the smaller is the suction. The range of the suction is approximately 1–6 kPa, which is approximately 0.20–0.42 when converted to volumetric water content using the soil water characteristic curve shown in Fig. 5. This result implies that the condition with a lower index has a higher potential risk of slope failure because the shear resistance decreases with decreasing suction.

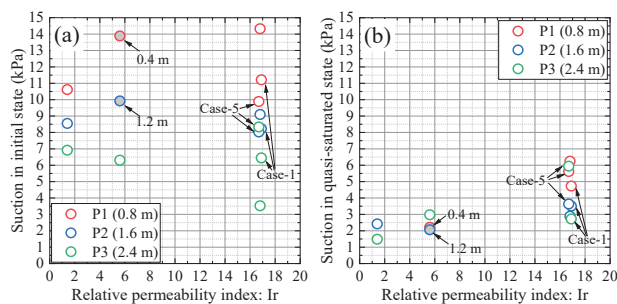


Fig. 6. Relationship between relative permeability index and suction in; (a) initial state, (b) quasi-saturated state.

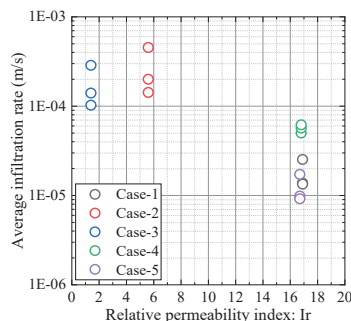


Fig. 7. Relationship between relative permeability index and average seepage velocity.

Fig. 7 shows the relationship between relative permeability index and average infiltration rate. The average infiltration rate was calculated by dividing the infiltration distance by the time required by the pore water pressure to start increasing again from the quasi-saturated state. The infiltration rate is high in Cases-2 and 3, whose index is low. The higher the infiltration rate, the shorter it takes for the slope to deform and the higher risk. With the same index, the infiltration rate of Case-4 is greater than that of Cases-3 and 5, which may be due to the effect of rainfall intensity.

### 3.3 Influence of Viscosity of Rainwater

Fig. 8 shows the comparison of the soil surfaces

immediately after spraying. Fine bubbles are formed on the surface when a viscous fluid is used. b However, as shown in Fig. 7, there is no significant difference in the infiltration rates of Case-5 using viscous fluid and Case-1 with the same apparent permeability. The suction in the quasi-saturated state shown in Fig. 6 (b) tends to be slightly higher when a viscous fluid is used, but the variation is large. A viscosity of approximately four times that of water, as in this case, did not have a significant effect on rainwater infiltration; however, the formation of bubbles may affect the infiltration at higher viscosities.



Fig. 8. Soil surfaces after spraying.

## 4 CONCLUSIONS

This paper presents the results of a series of vertical infiltration tests on uniform horizontal ground using a rainfall simulator in a centrifuge. The measurement of pore water pressure at each depth made it possible to understand rainwater infiltration into unsaturated sandy soil. It was found that there is a correlation between the relative permeability index and suction in the quasi-saturated state and infiltration rate. Further study on the influence of rainwater infiltration on slope deformation using a model slope in a centrifuge is necessary.

## ACKNOWLEDGEMENTS

The authors are grateful to Mr. Fujii and Mr. Tamaoka of Ehime University for conducting the centrifuge tests. This work was supported by JSPS KAKENHI (Grant Number JP21K14243).

## REFERENCES

- Iwata, N., Araki, Y., and Sasahara, K. 2014. Evaluation of shear deformation in granite soil slope due to rainfall based on field measurements, *Japanese Geotechnical Journal* 9(2): 141-151. (in Japanese)
- Kitamura, R. and Sako, K. 2010. Contribution of “Soils and Foundations” to studies on rainfall-induced slope failure. *Soils and Foundations* 50(6): 955-964.
- Koizumi, K., Oda, K., Komatsu, M., Ito, S., and Tsutsumi, H. 2019. Slope structural health monitoring method against rainfall-induced shallow landslide. *7th Int. Conference on Euro Asia Civil Engineering Forum* 615: 1-8.
- Tamate, S., Suemasa, N. and Katada, T. 2010. Simulation of precipitation on centrifuge models of slopes. *Int. J. Physical Modelling in Geotechnics* 12(3): 89-101.
- Zhang, G., Qian, J., Wang, R., and Zhang, J. 2011. Centrifuge model test study of rainfall-induced deformation of cohesive soil slopes. *Soils and Foundations* 51(2): 297-305.